



Incorporating Textile-Derived Cellulose Fibers for the Strengthening of Recycled Polyethylene Terephthalate for 3D Printing Feedstock Materials

Israel A. Carrete^{1,2} · Paulina A. Quiñonez^{1,2} · Diego Bermudez^{1,2} · David A. Roberson^{1,2}

Accepted: 22 September 2020 / Published online: 6 October 2020
© Springer Science+Business Media, LLC, part of Springer Nature 2020

Abstract

Unprecedented levels of production and consumption has led to solid waste accumulation in landfills and oceans. Two significant landfill constituents are textile waste and discarded plastic bottles. Since there is a finite amount of space available for landfill use, solutions that reuse these post-consumer products are imperative. The work presented here is a methodology for producing natural fiber-reinforced polymer composites (NFRPCs) from pseudo-raw materials. Post-consumer textile waste and polyethylene terephthalate (PET) water bottles were made compatible by way of surface modifications. Melt compounding was used to form a monofilament feedstock for extrusion-based 3D printing platforms. Hydrolysis and functionalization of cellulose fibers from white denim cloth was performed. It was found that adding recycled textile fibers to the recycled PET matrix had a toughening effect. Materials characterization involving dynamic mechanical analysis, attenuated total reflectance, impact testing, melt flow index, and scanning electron microscopy were carried out to verify the efficacy of the functionalization process and to ascertain the robustness of the filler/matrix interface. The outcome is a demonstration of a feasible method for the repurposing of waste products for 3D printing applications.

Keywords Fused deposition modeling · Plant fiber reinforcement · Additive manufacturing · Plastic recycling · Textile recycling

Introduction

Humankind's concern about post-consumer polymeric waste is rapidly growing as the environmental impact of discarded items becomes more and more obvious. As awareness of the impact of polymeric waste becomes more evident—considering the scale of the great oceanic garbage patches the size of the state of Texas [1]—several campaigns ranging from the municipal banning of plastic grocery bags, to the often berated banning of plastic drinking straws have arisen, indicating that attitudes concerning the environment are becoming less debatable and more accepted. Consumer

trends in the United States originated from a fear that a second Great Depression would occur if elevated production and consumption levels were not maintained in the post-war era [2]. Paired with advertisements that “psychologically conditioned” consumers into buying more, trends shifted from conservative practices to the consumerist practices that remain in place today [3]. As consumption increased, so did the accumulation of waste facilitated by planned obsolescence—the intentional premature failure of a product to promote repeat purchases [4–6]. In 2015, the United States generated 137.7 tons of solid waste, of which 26 million tons were plastics and 10.5 million tons were textiles; two constituents encouraged by single use consumption and planned obsolescence [7].

Current efforts to mitigate plastic waste accumulation vary and only account for small percentages of the total waste discarded. Of the 14 million tons of plastic discarded in the packaging industry in 2015, only 9% were recovered, whereas water bottles and jars saw a recycling rate of nearly 30% [7]. The remaining plastic waste has different endpoints, but a large portion of these end up in the

✉ David A. Roberson
droberson@utep.edu

¹ Polymer Extrusion Lab, The University of Texas at El Paso, El Paso, TX 79968, USA

² Department of Metallurgical, Materials and Biomedical Engineering, The University of Texas at El Paso, El Paso, TX 79968, USA

oceans, where wildlife is directly affected. With an estimated 4.8–12.7 metric tons of plastic entering the oceans in coastal regions alone [8], ocean surfaces are becoming covered by buoyant plastics. The oceanic currents break down relatively large plastic items into microplastic debris that can be fatal if ingested by marine wildlife [9]. The negative effects experienced by the wildlife that survive ingesting plastics are a consequence of the additive plasticizers found in the debris, which disrupt hormonal systems and affect the reproductive systems and development within these animals [10]. Furthermore, bacteria cannot easily decompose synthetic polymers, so humans that eat marine wildlife indirectly ingest these same microplastics, leading to reproductive health issues, damage to the endocrine systems of adolescents and adults and can also negatively influence fetal development [11]. Thus, inadequate management of plastic waste may easily evolve from an environmental issue to a medical one.

While the effects of plastic waste are well known because of masses such as the Great Pacific Garbage Patch, the analogous effects of textile waste; discarded clothing or other household textile items such as towels and bedding [12, 13], are less discussed. Fast fashion trends and improper disposal of textiles led to an accumulation of about 10.5 million tons of textiles in landfills in 2015 [7, 14]. This can be tied to the language surrounding fashion, which defines clothes as an extension of the owner and distracts from the reusability of nearly all textiles [15]. In 2015, for example, only 15% of textile waste was diverted from landfills because the owners ignored the different ways to recycle textiles [16]. The few cases where landfills are not the immediate destination of post-consumer clothes see them being donated or resold; often in developing nations [17].

In this work, we will use textile-derived cellulose to reinforce recycled thermoplastic material obtained from polyethylene terephthalate (PET) drinking water bottles. Here, we present a subset of a larger effort found in [18]. Cellulose has been used elsewhere as a filler as thermoplastic matrix composites and Mao and Hamad [19] highlighted the advantages of using cellulose as a reinforcing material including aspects such as biodegradability, abundance, low density, high specific strength, and CO₂ neutrality. Other researchers have utilized cellulose from waste streams to reinforce recycled thermoplastic materials. A recent work by Zander et al. [20] demonstrated the reinforcement of recycled polypropylene using cellulose derived from waste paper, cardboard and wood flower. Here the intended use was feedstock for FFF-type additive manufacturing platforms.

In other cases found in literature, 3D printing has also been utilized as an outlet for post-consumer polymeric waste. For example, another work by Zander et al. utilized recycled PET exclusively from water bottles with the intent of facilitating in-field manufacturing of plastic parts utilizing waste material [21]. Plant fibers have also been incorporated

into polymeric 3D printing feedstock, for example Torrado, et al. incorporated jute plant fiber from post-consumer rope into ABS feedstock in the creation of a polymer composite [22]. A detraction of using this plant fiber was that it combusted during the melt compounding and subsequent additive manufacturing process leading to the formation of voids in printed parts and to a decrease in mechanical strength. Milosevic et al. created a FDMTM-compatible composite from recycled polypropylene and plant fibers from hemp and harakeke [23], but did not realize a strength benefit from the plant fibers due to difficulty printing the composite material. The work presented here entails the conversion of PET drinking bottles into feedstock for FDMTM-type additive manufacturing platforms. In order to increase the strength of the recycled material, cotton fibers sourced from textiles were compounded with recycled PET. The result is a demonstration of repurposing two waste streams into usable feedstock material.

Materials and Methods

Unused PET drinking water bottles were obtained from Cordova Distributing Company (Cordova Distributing Company, LLC, El Paso, TX, USA). To facilitate converting the bottles into a form compatible with a thermoplastic extruder the tops and bottoms were removed cut into strips and then fed to a Fellowes 99Ms Micro-Cut Shredder. Shredding only with a cross shredder resulted in thin, confetti-like strips that easily tangled and prevented continuous feeding within a hopper, so these were introduced (along with the previously removed top and bottom of the bottle) into a Filabot Industrial Reclaimer (Filabot, Barre, VT, USA). The resulting granulated particles were then dried for 5 h at 150 °C in a compressed air dryer (Dri-Air CFAM Micro-Dryer, East Windsor, Connecticut, USA). The resulting pellet-like particles were extruded using a twin-screw extruder (Model ZK 25 T, Collin Lab and Pilot Solutions GmbH, Ebersberg, Germany) to obtain a uniform filament with a 1.75 mm diameter. Extrusion parameters are seen in Table 1.

To ensure controlled experiments, denim was sourced from Ted Pella, Inc. (Ted Pella Inc., Redding, CA, USA) in the form of lint-free cloths. The cloths were manually shredded through the use of a stainless-steel brush. The cloths with dimensions of 6" by 6" were attached to a small wooden block with screws to facilitate holding the cloth in one place as it was brushed on an 18" × 18" porcelain tile. Brushing occurred in the direction away from the wooden block to uniformly wear down the cloth and release small fibers. Fibers accumulated between the bristles of the brush and on the tile surface, where they were retrieved and placed in an aluminum container to avoid loss of the material due to electrostatic forces. In the creation of

Table 1 Extruder parameters for the recycled PET materials used in this study

| Zone | Zone 1 | Zone 2 | Zone 3 | Zone 4 | Zone 5 | Zone 6 | Pressure 1 (bar) | Extruder screws | Melt pump screws | Melt pump pressure | Feed rate |
|--------------|----------|----------|----------|----------|----------|----------|------------------|-----------------|------------------|--------------------|-----------|
| Value (unit) | 200 (°C) | 240 (°C) | 260 (°C) | 260 (°C) | 240 (°C) | 220 (°C) | 66 (bar) | 38–43 (rpm) | 12 (rpm) | 106–108 (bar) | 9 (%) |

any composite, adhesion between filler material and matrix material is important. Surface modifications induced by acid hydrolysis make hydrophilic cotton fibers compatible with a hydrophobic matrix, resulting in a natural fiber-reinforced polymer composite (NFRPC) [24–26]. We also desired to extract cellulose from the cotton fiber. To achieve both the extraction of the cellulose core from the cotton fibers and facilitate bonding between the cellulose and the PET polymer matrix a two-step hydrolysis/functionalization process was carried out on the fibers based on a procedure found in Araújo, et al. [27]. The process entailed exposure of 10 g of cotton fibers to an acid hydrolysis. The fibers were submerged in an acid solution containing 180 mL of distilled water, 20 mL of 98% (vol.) H₂SO₄ and 200 mL of 36% HCl and stirred for 150 min at 40 °C [27]. From this point, the suspension containing the fibers and solution were filtered using a vacuum filter and a Grade 5 Qualitative Filter Paper (GE Healthcare Life Sciences) until no liquid was left. The damp fibers were then placed in a beaker where a solution of 5% sodium bicarbonate (Arm & Hammer, USA) was added until a neutral solution was obtained. At this point, the suspension was washed in distilled water for 24 h before drying in a VWR Forced Air Oven (VWR International, Radnor, PA, USA) for 48 h. When dry, the suspension was removed from the oven and prepared to undergo the same acid hydrolysis process once more before being prepared for the silanization functionalization process. The silane used was (3-Aminopropyl)triethoxysilane (APTS) 98%; obtained from Sigma-Aldrich (Sigma-Aldrich, Inc., St. Louis, MO, USA). In this case, 1 gram of APTS was added to a 500 mL solution of 90% vol. ethanol to water. Once the cotton was added to the solution, the mixture was stirred for another 24 h at 60 °C, after which it was dried for 7 h at 80 °C. The resulting dry fibers exhibited some discoloration (the white fibers turned brown).

The PET granulate that was used to make a cellulose composite was also first dried at 150 °C for 5 h. Then, the fibers and pellets were manually mixed thoroughly in a beaker to give a 10 vol.% cotton-PET mixture. In this case, 100 mL of functionalized fibers were mixed with 900 mL of PET flakes. The homogeneity of the mixture facilitated a uniform distribution of fibers during the extrusion process. Additionally, it has been shown in other works by our group, that functionalization increases the dispersion of filler materials within a polymer matrix [28].

The small amount of the mixture necessitated the use of a desktop-grade single screw extruder. We could not use our twin screw extruder because the amount of material that would have been lost due to waste would have left us without enough material to fabricate test specimens. Here, a Filabot EX2 single-screw extruder was used at 250 °C and a screw speed at the highest possible value (slowly building up to it as pressure became uniform in the barrel). A 1.75 mm ±

0.15 mm diameter filament that was compatible with most desktop grade FFF 3D printers was extruded (Fig. 1). The photograph of spent impact test specimens (Fig. 1b) shows the color difference between recycled PET (RPET) and recycled PET-white cotton (RPET-WC) specimens.

All filaments were dried at 80 °C for 5 h in order to mitigate hygroscopic degradation within the filaments that may have occurred due to moisture absorption. Melt flow index (MFI) of the extruded materials was measured with a Tinius Olsen MP1200 Melt Flow Indexer (Tinius Olsen, Horsham, PA, USA). Further rheological studies of the materials studied here were carried out through Dynamic Mechanical Analysis (DMA). Specimens for DMA were printed with a Prusa i3 printer (Prusa Research, Czech Republic) and a crosshatched raster pattern of $\pm 45^\circ$ to the longitudinal axis of the specimen. All prints were carried out at a temperature of 260 °C, a print speed of 30 mm/s and an infill density of 100%. The DMA testing was performed on a Perkin Elmer DMA 8000 (PerkinElmer Waltham, MA, USA). Printed specimens for this test had the following dimensions: a length of 30 mm, width of 9 mm and thickness of 3 mm. A temperature scan was carried out in dual cantilever mode at a frequency of 1 Hz and dynamic force of 2N from 25 to 105 °C at a rate of 5°/min. The range of the scan was chosen arbitrarily around the reported glass transition temperature (T_g) for PET of 67 °C for amorphous PET and 81 °C for crystalline PET [18]. PerkinElmer Pyris TM software was used to analyze the information output by the instrument.

Izod pendulum impact tests were carried out on five specimens of each RPET and RPET-WC composites using a Tinius Olsen IT 504 polymeric impact testing machine (Tinius Olsen, Horsham, PA, USA). Specimens were printed in a cross-hatched raster pattern (raster directions in $\pm 45^\circ$) and the notch printed on top of the specimen, as proven by Roberson et al. [29] to be the most effective way to mimic a manufactured notch. The specimens were fabricated in accordance with the test geometry outlined in

ASTM D256-10 [30] and impact resistance (J/m), impact strength (J/m^2) and break energy (J) values were recorded. Tests were conducted with a drop height of 609.6 mm, a 15J pendulum capacity and an impact velocity of 3.46 m/s. The print parameters for the impact specimens were the same as the DMA specimens, but it is noted here that the specimens used for this test were printed with a 50% infill to conserve material.

Analysis via electron microcopy allowed for the understanding of how well the cotton fibers adhered to the PET matrix as well as characterization of fracture surfaces from impact tests and filament sections. Specimens were examined with a Hitachi SU3500 SEM (Hitachi High Technologies America, Irving, TX, USA) equipped with an ultra-variable detector (UVD) and operating with an accelerating voltage of 15 kV and a pressure of 60 Pa. The variable pressure mode was used to mitigate charge effects due to the non-conductive nature of the polymeric surfaces. Cross sections of the extruded filaments studied here were created by pulling the filament in tension until failure and both ends were viewed, along with a look at the transverse axis of the filament. Fractography was also conducted on representative impact specimens that most closely resembled the average values of the test set. As will be seen later, most of the specimens fractured completely after the test, so they had a fracture surface that could be analyzed to understand the behavior of crack propagation in these composites.

Results

Melt flow index measurements yielded results indicating the rheological changes induced by adding cotton-derived cellulose to recycled PET. Measurements of the baseline material, RPET, had the lowest MFI at 69.06 ± 9.892 g/10 min, whereas RPET-WC yielded an MFI value of 147.707 ± 33.831 g/10 min. We infer from the weight differences

Fig. 1 **a** Filament extruded from recycled PET and **b** spent impact test specimens where the lighter specimens are RPET and the darker specimens are the RPET-WC composite

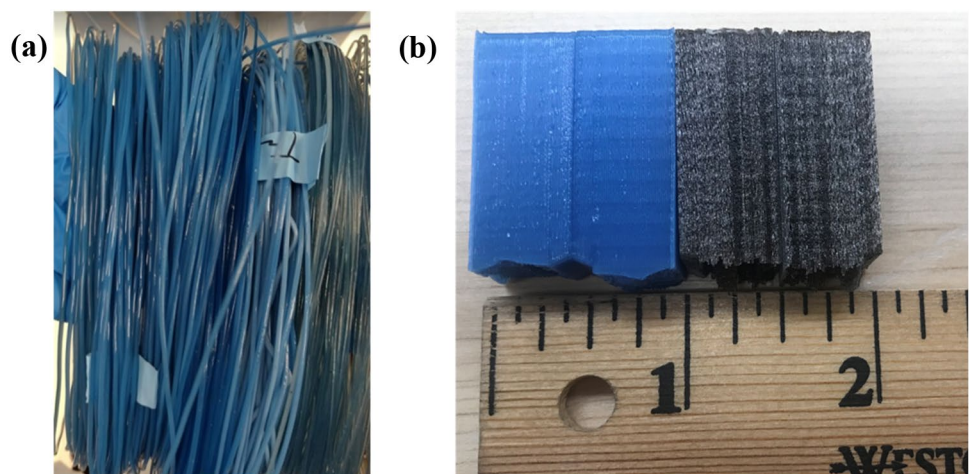
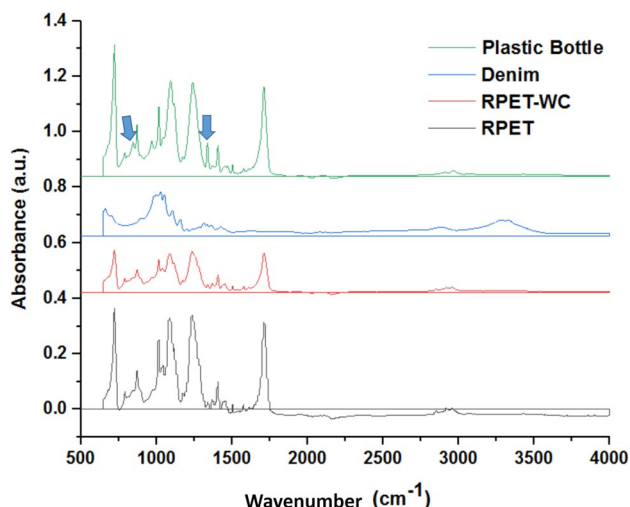


Table 2 MFI results for the filaments used in this study

| Material | MFI (g/10min) |
|-------------|------------------|
| RPET | 69.06 ± 9.892 |
| RPET 10% WC | 147.707 ± 33.831 |

**Fig. 2** ATR spectra

in MFI values that the addition of the hydrolyzed cotton fibers effectively lowered the viscosity of the RPET so that more material exited the MFI over the same time, temperature and weight conditions. The change in viscosity is most likely due to hydrolysis of the chemical (siloxane) bond between the matrix and fiber as was observed by Geng and Laborie [31] work on wood/thermoplastic composites. The MFI results for RPET and RPET loaded with 10% WC are presented in Table 2.

Attenuated total reflectance (ATR) was used to identify any chemical changes to the matrix or fibers induced by the compounding process. As seen in Fig. 2, the spectra for RPET, RPET-WC and an unprocessed plastic bottle are extremely similar where the peaks for the RPET-WC composite are somewhat suppressed. A notable difference observed when comparing the spectra from the unprocessed bottle and the extruded materials is evident at 1400 and 833 cm^{-1} (indicated by arrows), as these peaks are not present in the spectra for the RPET nor the RPET-WC composites, indicating that the extrusion process is breaking polymeric

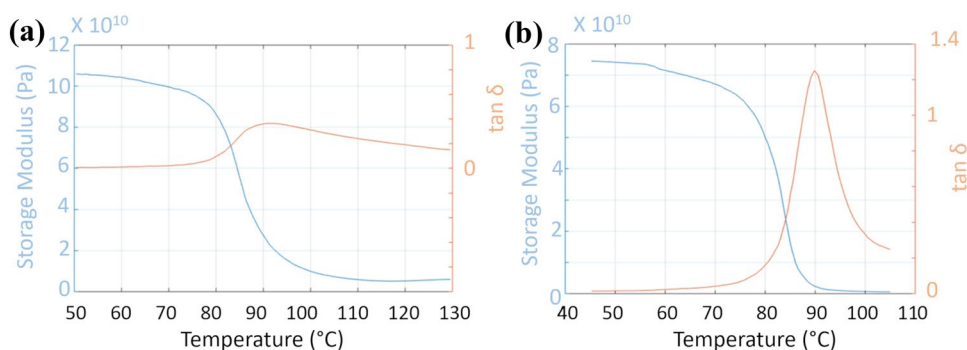
bonds and degrading the material somewhat. Altering the chemical bonds in the polymer matrix would be expected due to the effect of thermomechanical degradation induced by the extrusion process [32, 33]. Cellulose, which would be identified by peaks between 2800 and 3000 cm^{-1} [27] appears as a broad curve on the spectra for the denim sheet and the presence of cellulose in the RPET composite may be responsible for the morphological differences in the peaks at that location when compared to the unfilled RPET. The difference in peak morphology at 1175 cm^{-1} on the RPET-WC spectra could potentially be representative of silanization as the peak differs from the RPET and plastic bottle spectra. This peak is indicative of new bonds created by the functionalization process [18].

Analysis via DMA for RPET and RPET-WC were carried out on three specimens of each material type. The average values for glassy onset based on storage modulus drops and the max tan delta are presented in Table 3, while representative curves of the DMA tests are seen in Fig. 3. As can be seen in the table, the value of storage moduli at the onset of glassy behavior were $8.86 \times 10^{10} \pm 1.12 \times 10^{10}$ Pa and $6.58 \times 10^{10} \pm 0.34 \times 10^{10}$ Pa for RPET and RPET-WC, respectively. The decrease in storage modulus values along with a slight drop in onset temperature (78.59 °C and 77.40 °C for RPET and RPET-WC, respectively) suggests again, that the chemical bond between fiber and matrix was subject to hydrolysis and agrees with the results of the MFI measurements. The dampening capacity of the material system was increased with the addition of cotton fibers as indicated by the max loss tangent (tan δ) values and the temperatures at which the maximum tan δ occurred. The temperature where the tan δ curve was greatest increased from 86.99 for RPET to 89.18 °C for RPET-WC. Overall, this creates a widening of the transition from glassy to rubbery behavior, giving a larger range of temperatures between which thermal processing can occur. Finally, the max tan δ value at these points increased from 0.28 ± 0.14 for RPET to 1.34 ± 0.09 for the RPET-WC composite. The increase in tan δ , suggests that the addition of cotton fibers improves the ability of the material to dampen impact, often associated with a better dissipation of energy, or impact resistance at the expense of elasticity [34, 35].

Five impact tests were printed for both the RPET and RPET-WC materials. The average values of these tests are shown in Table 4. As expected from the DMA results,

Table 3 Tabularized DMA data

| Material | Storage modulus | | Loss tangent | | |
|----------|---|------------|------------------|-----------|------------|
| | Glassy onset (Pa) | Temp. (°C) | Max tan δ | FWHM (°C) | Temp. (°C) |
| RPET | $8.86 \times 10^{10} \pm 1.12 \times 10^{10}$ | 78.59 | 0.28 ± 0.14 | 25.3 | 86.99 |
| RPET-WC | $6.58 \times 10^{10} \pm 0.34 \times 10^{10}$ | 77.40 | 1.34 ± 0.09 | 8.2 | 89.18 |

Fig. 3 DMA curves for **a** RPET and **b** the RPET-WC composite

a toughening effect is evident in the cotton specimens given that the impact resistance and impact strength were increased from 14.4 ± 2.58 to 23.3 ± 5.21 J/m and 1384 ± 244 to 2268 ± 501 J/m², respectively. The higher energy needed to break the specimens is indicative of more ductile behavior that dissipates impact energy more effectively. In other words, the addition of functionalized cotton fibers is toughening or even plasticizing the RPET matrix. It is worth mentioning as well, that, while RPET fractured completely in a brittle manner, the increased ductility of adding cotton led to incomplete fracture of two of the RPET-WC composite specimens. The upper half of the specimen was left hanging even after impact resulting in a “hinge” failure. Recalling that fiber orientation affects mechanical properties, it is possible that, because the beads are drawn in one direction, the fibers align with printing direction. Since these specimens were printed in a cross-hatched raster pattern, the fiber reinforcement would then have a coincident orientation; improving toughness. SEM images of representative fracture surfaces for each material support this hypothesis.

The scanning electron micrograph in Fig. 4 shows the fracture surface near the v-notch interface of a representative specimen printed from RPET feedstock. At the interface, interlayer adhesion is clear as the individual beads are indistinguishable, unlike those seen in the subsequent layers (Indicated by the arrow in Fig. 4a). Since these samples were printed at 50% infill, interlayer bonding did not homogenize the structure and the individual layers are easily distinguishable. Multiple fracture features are observable that are consistent with brittle mode failure. The higher magnification image (Fig 4b) exhibits a large number of smooth “mirror” fracture surface features (indicated by solid white arrow) indicative of a brittle mode failure [36]. Hackle lines are also seen (highlighted by dashed arrow) adjacent to the smooth

fracture features. The fracture surface also indicates that the extruded filament was of good quality as no voids are readily visible in the cross-section.

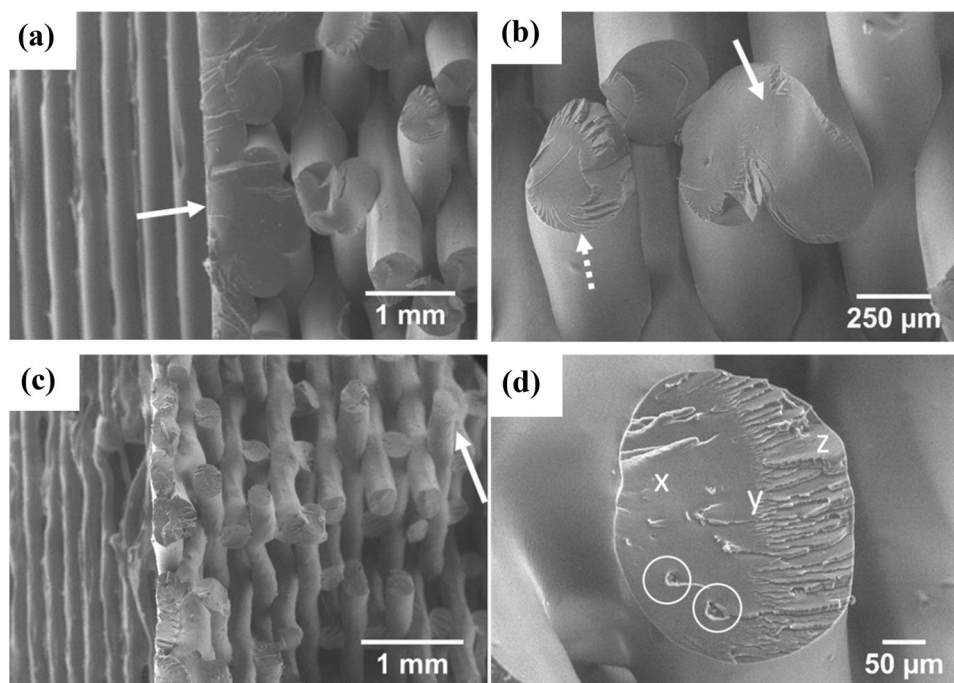
In contrast, the electron micrographs displayed in Fig. 4c, d indicates a different morphology near the v-notch interface for the RPET-WC specimen. Despite having the same printing parameters, the beads with cotton fiber appear to be thinner with a roughness to the surface. The thinner beads are due to the lower viscosity of the material while integration of cellulose fibers in the matrix led to the surface roughness. Based on the MFI data, the printing parameters should have been altered to account for differences in rheological behavior. The higher magnification micrograph (Fig. 4d) exhibits a large mirror section along with a mist and hackle region (indicated by x, y, z respectively) transitioning into the fracture along the propagation of the crack. However, unlike the mainly smooth surfaces of RPET impact specimens, those from RPET-WC possess regions where the cotton fibers helped resist the impact (indicated by circles on Fig. 4d). Additionally, the material was more ductile than the RPET alone as indicated by the necking feature highlighted by white arrow in Fig. 4c. Despite the shear deformation zones surrounding the fibers, there are no voids present, indicating that proper adhesion between the matrix and fibers occurred and energy dissipation is taking place. The larger deformation present in the RPET-WC specimens agrees well with the recorded impact test, DMA and MFI results discussed earlier. As was the case with the unloaded RPET filament, micrographs of the composite RPET-WC filament did indicate the presence of voids further indicating that the compounding process yielded a low-defect filament.

In order to further evaluate the extruded filament, small filament sections of the two extruded materials were

Table 4 Impact test data

| Material | Impact resistance (J/m) | Impact strength (J/m ²) | Impact break energy (J) |
|----------|-------------------------|-------------------------------------|-------------------------|
| RPET | 14.38 ± 2.579 | 1384 ± 243.988 | 0.1792 ± 0.033 |
| RPET-WC | 23.3 ± 5.210 | 2268 ± 501.318 | $0.2872 \pm .064$ |

Fig. 4 Electron micrographs of spent Izod impact test specimens where **a** is at the root of the stress-concentrating notch on the RPET specimen and **b** is a higher mag image in the bulk of the fracture surface. The impact specimen composed of the RPET-WC composite shown in **c** exhibits necking on the print beads, while in **d** x, y, and z corresponds with mirror, mist and hackle regions



manually pulled along the longitudinal axis until failure in order to create a fracture surface indicative of the material's response to tension. Though this was not a controlled process, the resulting fracture surfaces were still able to be examined. The electron micrograph seen in Fig. 5 is of matching fracture surfaces of a section of RPET filament. Similar to observations made on the impact test specimen, the filament fracture surface exhibits a brittle mode failure with the characteristic mirror, mist and hackle marks, however, the crack propagation was in a spiral pattern (Fig 5a). The slightly higher magnification (Fig. 5b) exhibits hackle marks that propagated in several directions (indicated by arrows). There is little to no observable plastic deformation indicating a lack of plasticity for the material. The findings from this manually-induced failure correlate well with the rheological and impact testing conducted on the RPET material.

Once white cotton fibers were added to the matrix, there was a different response to stress and the fracture surface

changed significantly. Unlike RPET, RPET-WC underwent significant plastic deformation indicated by necking (white arrow in Fig. 6a) which is consistent with the other characterization methods used in this study. Plastic deformation surrounding small circular artifacts (circled in the figure) likely occurred with the pullout of fibers below the critical aspect ratio [37]. The lower portion exhibits much larger voids resulting from strain fields that manifested during the deformation process [34] and the cusp like morphology of the bottom of the strain field can be seen (Fig. 6b). Though it is possible that the strain fields were induced by the presence of small portions of the cellulose particles, overall, the composite shows robust adhesion. The fibers seen on the surface of the filament were properly incorporated into the matrix and there was no significant evidence to show that poor adhesion led to stress concentration and eventual causality of the fracture. The micrographs in Fig. 6c, d are of the mating surface to those seen Fig. 6a, b, and exhibit fiber pullout, which would normally indicate poor fiber/matrix

Fig. 5 Fracture surfaces of a RPET filament manually pulled in tension to failure where **a** indicates the spiral nature of the crack propagation and **b** indicates the multiple directions of hackle mark orientations

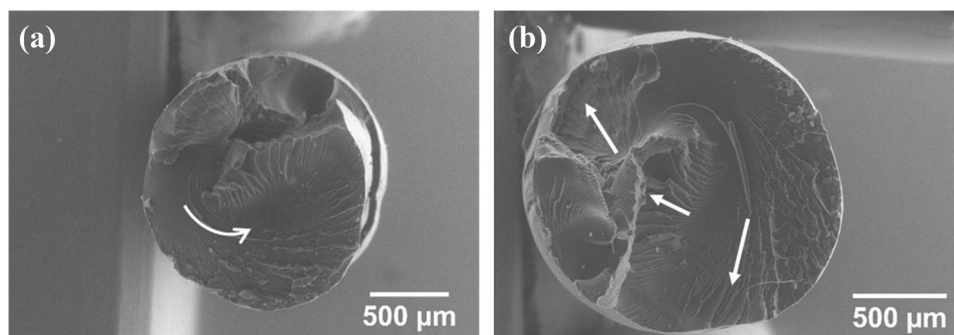
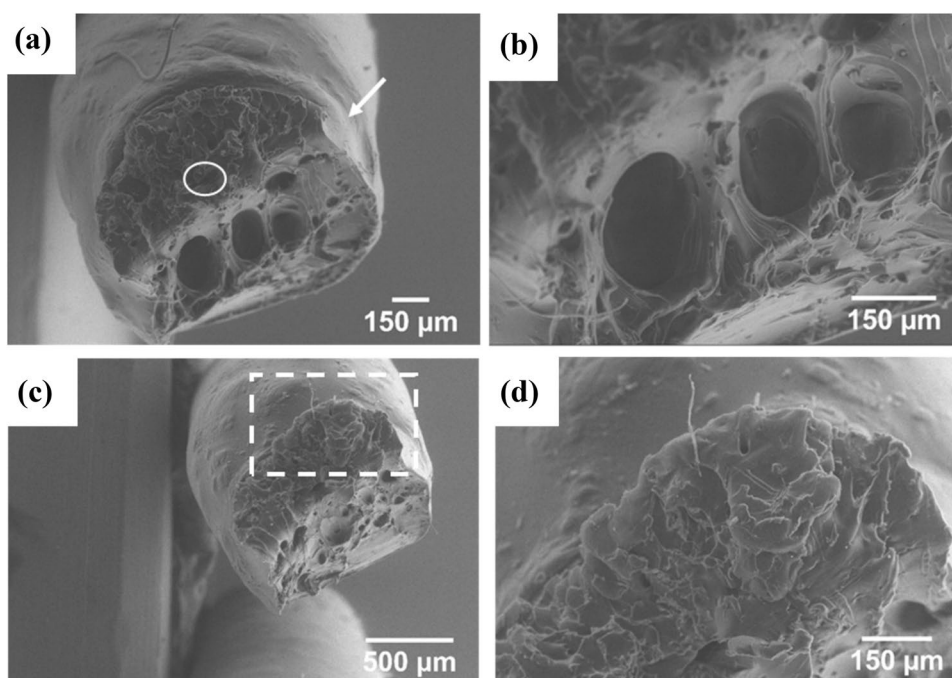


Fig. 6 **a** Electron micrograph of a fracture surface of a RPET-WC composite filament where necking and fiber pullout are indicated by an arrow and oval, respectively and large strain fields are seen in the higher magnification image, **b** The fracture surface of the RPET-WC composite filament where **c** is a low mag image and **d** is a higher mag image of a fiber that experienced pullout and exhibits evidence of buckling

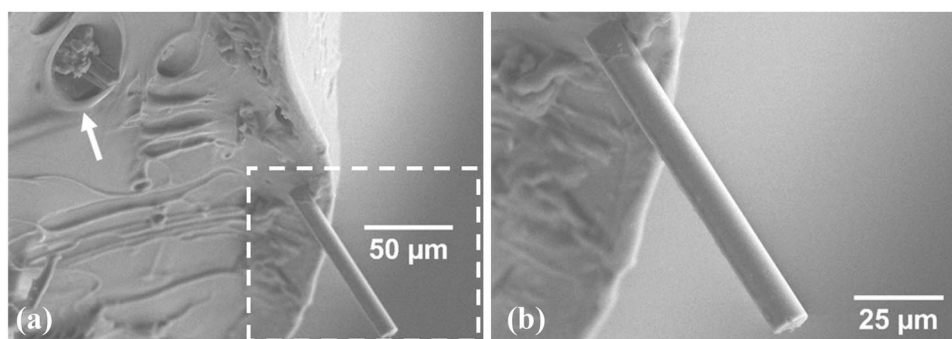


adhesion, but the presence of necking and large amount of plastic deformation make it difficult to claim that the fibers de-bonded from the matrix prior to material yielding. The instance of fiber pullout (highlighted by the white square in Fig. 6c) is proof that stress was properly transferred to the fiber from the matrix in deformation. The higher magnification image of the fiber (Fig. 6d) shows the fiber has buckled indicating that the fiber was subjected to a considerable amount of force.

The electron micrograph in Fig. 7 clearly depicts the morphology of the cellulose fiber that pulled out of the matrix upon material failure. In this case, the fiber shows little to no amorphous regions. We are associating the morphology of the fiber as an indicator of the crystalline nature of the fiber. This microcrystalline cellulose structure is typical of a fiber that has been hydrolyzed to the point that the amorphous region is no longer visible, which benefits the mechanical properties of the fiber [38, 39]. With a diameter in the range

of 10 μ m, the base of the fiber (Fig 7b) shows no signs of voids, meaning that interfacial adhesion between matrix and fiber are appropriate to transfer stress onto the fiber. However, the small circular voids are signs of strain fields caused by the presence of the fiber (indicated by white arrow in Fig. 7a). Overall, the functionalization of cotton produced a natural fiber reinforced composite with appropriate adhesion between components, but the hydrolyzation of cotton fibers was not uniform, as the extent of amorphous material present varied as not all of the fibers observed had the crystal-like morphology observed in Fig 7. Cotton fibers have a high specific strength, with a tensile strength in the range of 287–597 MPa despite their low density (1.5 g/cm) [40]. The strengthening effect was realized when comparing the impact resistance data between RPET and the RPET-WC composite. Additionally, the addition of fibers changes the fracture mode of the filament from a brittle to a largely ductile mode.

Fig. 7 Electron micrograph of a RPET-WC filament. The white arrow in **a** indicates a strain field that manifested around the fiber prior to rupture. **b** is the high mag of the area outlined in white dashes in **a**



Summary and Conclusions

The surge of polymer extrusion-based additive manufacturing technologies over the last decade serves as an opportunity to create new material systems that may benefit society either through novel material systems or by providing a way to produce composite materials out of consumer waste streams. The latter is explored in this study with the hope of tackling two large contributors to solid waste: (1) cotton from textiles; and (2) polymeric waste from drinking bottles. As a proof of concept, the study presented here shows that creating a natural fiber-reinforced polymer composite (NFRPC) from recycled PET combined with cellulose sourced from recycled denim textile has a positive effect on impact resistance and the dampening characteristics. The two materials were repurposed and combined to make a composite feedstock material for polymer extrusion-based additive manufacturing technologies such as fused deposition modeling (FDM™). The surface modifying techniques of acid hydrolysis and silane functionalization were carried out with the intent to make the cotton fibers compatible with a recycled PET (RPET) matrix.

Characterization of the filament types through attenuated total reflectance (ATR) showed that functionalization chemically changed the cotton fibers for the benefit of adhesion to the RPET matrix. Mixing in the extruder also altered the RPET matrix, as some peaks that were present in non-processed PET no longer appeared in either filament. Furthermore, melt flow index (MFI) measurements hinted at a plasticizing effect of the fibers on the matrix as the composite had a higher MFI than the matrix, potentially indicating that some damage the siloxane bond between the fiber and polymer had occurred. Dynamic mechanical analysis (DMA) results agreed with the MFI measurements as the storage modulus at glassy onset was lower for the RPET-WC composite as compared to the specimens fabricated from RPET alone.

Fractography via SEM revealed a brittle fracture mode for RPET and a ductile mode for the RPET-WC composite. Izod impact test results confirmed that the incorporation of hydrolyzed cotton fibers led to a toughening effect as indicated by higher impact resistance values. SEM images of impact fracture surfaces revealed that fiber-matrix adhesion was robust as signs of fiber pullout were minimal.

The work explored here serves a template for the combination of waste streams in the creation of feedstock material for additive manufacturing processes. However, there is still much work that can be done to make the process more marketable at a large scale, which is why further research in innovative recycling methods is imperative. The methodologies presented here will not only aid in

the decrease of waste, but allow for the manufacturing of robust, polymeric parts in austere environments and other locales with limited resources.

Acknowledgements The work demonstrated in this article was carried out in the Polymer Extrusion Lab in the Department of Metallurgical, Materials and Biomedical Engineering at The University of Texas at El Paso. The authors thank Ing. Gustavo Cordova of Cordova Distributing, LLC for his donation of drinking water bottles.

References

- Kaiser J (2010) The dirt on ocean garbage patches. *Science* 328:1506. <https://doi.org/10.1126/science.328.5985.1506>
- Blumberg L, Gottlieb R (1989) *War on waste: can america win its battle with garbage?* Louis Blumberg Robert Gottlieb. Island Press, Washington
- Guiltinan J (2009) Creative destruction and destructive creations: environmental ethics and planned obsolescence. *J Bus Ethics* 89:19–28. <https://doi.org/10.1007/s10551-008-9907-9>
- Packard V (1959) *The status seekers an exploration of class behavior in America*. Longmans, New York
- Aladeojebi TK (2013) Planned obsolescence. *Int J Sci Eng Res* 6:1504–1508
- Mason R (1985) Ethics and the supply of status goods. *J Bus Ethics* 4:457–464. <https://doi.org/10.1007/BF00382607>
- US EPA (2015) US EPA, National overview: facts and figures on materials, wastes and recycling
- Jambeck JR, Geyer R, Wilcox C et al (2015) Marine pollution. Plastic waste inputs from land into the ocean. *Science* 347:768–771. <https://doi.org/10.1126/science.1260352>
- Thompson RC (2006) Plastic debris in the marine environment: consequences and solutions. In: *Marine Nature Conservation in Europe 2006*. Stralsund, Germany
- Fries E, Dekiff JH, Willmeyer J et al (2013) Identification of polymer types and additives in marine microplastic particles using pyrolysis-GC/MS and scanning electron microscopy. *Environ Sci Process Impacts* 15:1949. <https://doi.org/10.1039/c3em00214d>
- Liboiron M (2016) Redefining pollution and action: the matter of plastics. *J Mater Cult* 21:87–110. <https://doi.org/10.1177/1359183515622966>
- Koch K, Domina T (1997) The effects of environmental attitude and fashion opinion leadership on textile recycling in the US. *J Consum Stud Home Econ* 21:1–17. <https://doi.org/10.1111/j.1470-6431.1997.tb00265.x>
- Domina T, Koch K (1997) The textile waste lifecycle. *Cloth Text Res J* 15:96–102. <https://doi.org/10.1177/0887302X9701500204>
- Claudio L (2007) Waste couture: environmental impact of the clothing industry. *Environ Health Perspect*. <https://doi.org/10.1289/ehp.115-a449>
- Lewis T (2015) Apparel disposal and reuse. *Sustain Appar*. <https://doi.org/10.1016/B978-1-78242-339-3.00010-8>
- Binotto C, Payne A (2017) The poetics of waste: contemporary fashion practice in the context of wastefulness. *Fash Pract* 9:5–29. <https://doi.org/10.1080/17569370.2016.1226604>
- Norris L (2012) Trade and transformations of second-hand clothing: introduction. *Textile* 10:128–143. <https://doi.org/10.2752/175183512X13315695424473>
- Carrete IA (2019) Development and characterization of polyethylene terephthalate (PET)-cotton natural fiber-reinforced composites from waste materials. The University of Texas at El Paso, El Paso

19. Miao C, Hamad WY (2013) Cellulose reinforced polymer composites and nanocomposites: a critical review. *Cellulose* 20:2221–2262
20. Zander NE, Gillan M, Burckhard Z, Gardea F (2019) Recycled polypropylene blends as novel 3D printing materials. *Addit Manuf* 25:122–130. <https://doi.org/10.1016/j.addma.2018.11.009>
21. Zander NE, Gillan M, Lambeth RH (2018) Recycled polyethylene terephthalate as a new FFF feedstock material. *Addit Manuf* 21:174–182. <https://doi.org/10.1016/j.addma.2018.03.007>
22. Torrado AR, Roberson DA (2016) Failure analysis and anisotropy evaluation of 3D-printed tensile test specimens of different geometries and print raster patterns. *J Fail Anal Prev* 16:154–164. <https://doi.org/10.1007/s11668-016-0067-4>
23. Milosevic M, Stoff D (2017) Characterizing the mechanical properties of fused deposition modelling natural fiber recycled polypropylene composites. *J Compos Sci* 1:7. <https://doi.org/10.3390/jcs1010007>
24. Azizi Samir MAS, Alloin F, Dufresne A (2005) Review of recent research into cellulosic whiskers, their properties and their application in nanocomposite field. *Biomacromolecules* 6:612–626. <https://doi.org/10.1021/bm0493685>
25. Dong XM, Revol J-F, Gray DG (1998) Effect of microcrystallite preparation conditions on the formation of colloid crystals of cellulose. *Cellulose* 5:19–32. <https://doi.org/10.1023/A:1009260511939>
26. Medeiros ES, Mattoso LHC, Bernardes-Filho R et al (2008) Self-assembled films of cellulose nanofibrils and poly(o-ethoxyaniline). *Colloid Polym Sci* 286:1265–1272. <https://doi.org/10.1007/s00396-008-1887-x>
27. Araújo RS, Ferreira LC, Rezende CC et al (2018) Poly(lactic acid)/cellulose composites obtained from modified cotton fibers by successive acid hydrolysis. *J Polym Environ* 26:3149–3158. <https://doi.org/10.1007/s10924-018-1198-3>
28. Roberson David, Shemelya Corey M, MacDonald Eric, Wicker Ryan (2015) Expanding the applicability of FDM-type technologies through materials development. *Rapid Prototyp J* 21:137–143. <https://doi.org/10.1108/RPJ-12-2014-0165>
29. Roberson DA, Torrado Perez AR, Shemelya CM et al (2015) Comparison of stress concentrator fabrication for 3D printed polymeric izod impact test specimens. *Addit Manuf* 7:1–11. <https://doi.org/10.1016/j.addma.2015.05.002>
30. D20 Committee Test Methods for Determining the Izod Pendulum Impact Resistance of Plastics
31. Geng Y, Laborie M-PG (2010) The impact of silane chemistry conditions on the properties of wood plastic composites with low density polyethylene and high wood content. *Polym Compos* 31:897–905. <https://doi.org/10.1002/pc.20873>
32. Najafi SK, Mostafazadeh-Marznaki M, Chaharmahali M, Tajvidi M (2009) Effect of thermomechanical degradation of polypropylene on mechanical properties of wood-polypropylene composites. *J Compos Mater* 43:2543–2554. <https://doi.org/10.1177/0021998309345349>
33. Steward EL, Bradley M (1991) The influence of extrusion parameters on the degradation of polypropylene. *J Plast Film Sheeting* 7:355–374. <https://doi.org/10.1177/875608799100700407>
34. Carrete IA, Bermudez D, Aguirre C et al (2019) Failure analysis of additively manufactured polyester test specimens exposed to various liquid media. *J Fail Anal Prev*. <https://doi.org/10.1007/s11668-019-00614-0>
35. Menard KP, Bilyeu BW (2008) Dynamic mechanical analysis of polymers and rubbers. In: *Encyclopedia of analytical chemistry*. Wiley, Chichester
36. Shemelya CM, Rivera A, Perez AT et al (2015) Mechanical, electromagnetic, and X-ray shielding characterization of a 3D printable tungsten-polycarbonate polymer matrix composite for space-based applications. *J Electron Mater* 44:2598–2607. <https://doi.org/10.1007/s11664-015-3687-7>
37. Schnittker K, Arrieta E, Jimenez X et al (2018) Integrating digital image correlation in mechanical testing for the materials characterization of big area additive manufacturing feedstock. *Addit Manuf*. <https://doi.org/10.1016/j.addma.2018.12.016>
38. Das K, Ray D, Bandyopadhyay NR et al (2009) A study of the mechanical, thermal and morphological properties of microcrystalline cellulose particles prepared from cotton slivers using different acid concentrations. *Cellulose* 16:783–793. <https://doi.org/10.1007/s10570-009-9280-6>
39. Haafiz MKM, Hassan A, Zakaria Z et al (2013) Properties of polylactic acid composites reinforced with oil palm biomass microcrystalline cellulose. *Carbohydr Polym* 98:139–145. <https://doi.org/10.1016/J.CARBPOL.2013.05.069>
40. Li X, Tabil LG, Panigrahi S (2007) Chemical treatments of natural fiber for use in natural fiber-reinforced composites: a review. *J Polym Environ* 15:25–33. <https://doi.org/10.1007/s10924-006-0042-3>

Publisher's Note Springer Nature remains neutral with regard to jurisdictional claims in published maps and institutional affiliations.